Science of the Total Environment 621 (2018) 444–452

Contents lists available at ScienceDirect

Science of the Total Environment

journal homepage: www.elsevier.com/locate/scitotenv

Simulating emissions of 1,3-dichloropropene after soil fumigation under field conditions

S.R. Yates [a,*], D.J. Ashworth [a,b]

[a] USDA-ARS, U.S. Salinity Laboratory, 450 W. Big Springs Rd., Riverside, CA 92507, United States
[b] University of California, Department of Environmental Sciences, Riverside 92521, United States

HIGHLIGHTS

- Compares predicted and measured fumigant emissions from five field experiments
- Two independent datasets and five methods were available for measured emissions.
- Total emissions were adequately predicted using a standard modeling approach.
- The ranges of predicted and measured emissions were similar (5.8–29% and 4.3–26%).

GRAPHICAL ABSTRACT

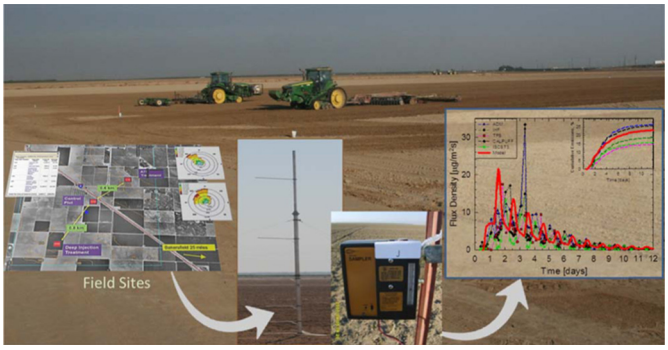

ARTICLE INFO

Article history:
Received 28 September 2017
Received in revised form 22 November 2017
Accepted 24 November 2017
Available online xxxx

Editor: Jay Gan

Keywords:
Soil fumigation
Volatilization
Emissions
Modeling
1,3-Dichloropropene

ABSTRACT

Soil fumigation is an important agricultural practice used to produce many vegetable and fruit crops. However, fumigating soil can lead to atmospheric emissions which can increase risks to human and environmental health. A complete understanding of the transport, fate, and emissions of fumigants as impacted by soil and environmental processes is needed to mitigate atmospheric emissions. Five large-scale field experiments were conducted to measure emission rates for 1,3-dichloropropene (1,3-D), a soil fumigant commonly used in California. Numerical simulations of these experiments were conducted in predictive mode (i.e., no calibration) to determine if simulation could be used as a substitute for field experimentation to obtain information needed by regulators. The results show that the magnitude of the volatilization rate and the total emissions could be adequately predicted for these experiments, with the exception of a scenario where the field was periodically irrigated after fumigation. In addition, the timing of the daily peak 1,3-D emissions was not accurately predicted for these experiments due to the peak emission rates occurring during the night or early-morning hours. This study revealed that more comprehensive mathematical models (or adjustments to existing models) are needed to fully describe emissions of soil fumigants from field soils under typical agronomic conditions.

1. Introduction

Soil fumigant chemicals have the potential to increase atmospheric concentration of photochemical smog precursors, which could react with nitrogen oxides in the atmosphere and can significantly impact regional air quality by emitting toxic substances into the regional air

* Corresponding author.
E-mail address: scott.yates@ars.usda.gov (S.R. Yates).

https://doi.org/10.1016/j.scitotenv.2017.11.278
0048-9697/

stream (van den Berg et al., 1999; Yates et al., 2011b). Photochemical smog has become a problem in California during the summer months and fumigants have been identified as potential contributors. Monitoring indicates that additional efforts are needed to ensure that U.S. EPA's 8-h ozone standard is attained throughout the state (Neal et al., 2009).

Telone II® (1,3-dichloropropene, 1,3-D) is an effective nematicide commonly used for preplant soil fumigation. According to CDPR (2017), 1,3-D was the most highly used fumigant (based on mass applied) in CA from 2011 to 2015 and the third most highly used pesticide (based on mass applied) in 2015. Between 2007 and 2015, 1,3-D use in CA increased from 4.3 × 106 kg (9.5 × 106 lbs) to 7.2 × 106 kg (15.8 × 106 lbs), with the applied land area increasing from 21.8 × 103 ha (53.9 × 103 acres) to 32.2 × 103 ha (79.4 × 103 acres). However, 1,3-D is considered a possible carcinogen and is a Clean Air Act substance (Baker et al., 1996). The high volatility of 1,3-D (vapor pressure 4.3 kPa; Wauchope et al., 1992) facilitates its movement (which increases effectiveness), but can also lead to high atmospheric emissions and the potential for worker exposure (Albrecht, 1987). In 1990, the detection of high 1,3-D concentrations in ambient air samples at multiple sites in California led to a temporary suspension of 1,3-D as a soil fumigant (CDPR, 2002). The suspension remained in effect until 1995 when approaches to mitigate emissions were developed and tested.

There is very little published information on field-scale emissions of 1,3-D. There have been several reported soil column experiments (Basile et al., 1986; Gan et al., 1998a, 1998b; Zheng et al., 2006; Gao and Trout, 2007; McDonald et al., 2008; Ashworth et al., 2009) that placed 1,3-D emission losses from bare soil in the range 20–77% of the applied dosage. These studies also revealed that emission rates obtained using laboratory soil columns can have high variability (i.e., $\mu = 41\%$, $\sigma = 16\%$). Total emission rates have been obtained under field conditions using micrometeorological and flux chamber methods. These studies have shown a similar range in total emissions 12–80% (van den Berg, 1992; Chen et al., 1995; van Wesenbeeck et al., 2007; Chellemi et al., 2010; Gao et al., 2008; Gao et al., 2009), with the highest estimates obtained using flux chambers ($\mu = 56\%$, $\sigma = 22\%$). Flux chambers offer a relatively simple and cost-effective method for determining emission rates. They are also known to suffer from several practical problems such as sampling a small surface area and the presence of the chamber affecting the tested surface (Gao et al., 1997), which can affect the emission measurements. Flux chambers have been shown to provide results consistent with micrometeorological methods when flux chambers are well designed and appropriately used (Gao et al., 1997). Flux chambers may be the only practical method available for measuring emissions for small treated areas or when experiments are conducted with several treatments in close proximity.

It is important to understand emissions from fumigated soil at typical agronomic-scales to reduce the adverse impacts from soil fumigation. Large-scale field measurement of fumigant emissions provides information regulators require at the appropriate scale while serving as a reference baseline for the development and testing of new methods to reduce emissions.

Continued use of soil fumigant chemicals in the future will likely require developing strategies to reduce emission rates. In order to achieve this goal, extensive environmental fate and transport information is needed that can be used to design and test potential mitigation approaches compatible with large farming operations. However, field experimentation is expensive and comparing the results from different field experiments is tenuous unless the experiments are conducted at the same time, in the same location and in the same (or similar) soil type. Meeting these requirements significantly increases the cost and complexity of field experimentation.

Computer modeling provides an alternative to conducting large-scale field experiments. Using modeling, new and potentially cost-effective management practices could be developed and initially tested by comparing simulation results from new vs. standard pesticide management methods. Potential fumigation practices that mitigate emissions could then be tested in the field. However, before this type of approach becomes useful, it is necessary to understand and be able to predict all of the important routes of transport and dissipation, so that models outputs are similar to field measurements.

The objective of this study was to determine if numerical simulation can be used as a substitute for conducting complex, expensive and time consuming 1,3-D field experiments. Field experiments are currently used to quantify regulatory information on the short-term and total emission rates of 1,3-D after shank fumigation in large-scale agricultural fields. Information on emissions is required by state and federal regulators as inputs into risk assessment models for the development of buffer zones to ensure public safety, and also benefits the agricultural community by providing science-based information concerning rates of emission. The simulation results described below were obtained in a predictive mode and did not use any inverse approach.

2. Modeling methods

2.1. Transport equations

The model used to simulate fumigant fate and transport in variably-saturated soils and subject to variable temperatures requires three governing processes: water flow, heat transport, and solute fate and transport. The transport of water was simulated using Richard's Equation (Šimůnek and van Genuchten, 1994; Jury and Horton, 2004):

$$\frac{\partial \theta}{\partial t} = \frac{\partial}{\partial x}\left[K_x(h)\frac{\partial h}{\partial x}\right] + \frac{\partial}{\partial z}\left[K_z(h)\frac{\partial h}{\partial z} + K_z(h)\right] - S \quad (1)$$

where θ is the volumetric water content ($cm^3\ cm^{-3}$), h is the pressure head (cm), K is hydraulic conductivity ($cm\ s^{-1}$), and S is a sink term (s^{-1}); t is time (s), x and z is distance (cm). For all simulations, the sink term was set to zero.

Heat transport was simulated using Eq. (2) (Šimůnek and van Genuchten, 1994):

$$C_h(\theta)\frac{\partial T}{\partial t} = \frac{\partial}{\partial x}\left[\lambda_x(h)\frac{\partial T}{\partial x}\right] + \frac{\partial}{\partial z}\left[\lambda_z(h)\frac{\partial T}{\partial z}\right] - C_w q\frac{\partial T}{\partial z} \quad (2)$$

where T is soil temperature (K), C_h and C_w are the volumetric heat capacity for the porous media ($J\ m^{-3}\ K^{-1}$) and liquid, respectively, and λ is the apparent thermal conductivity ($W\ m^{-1}\ K^{-1}$).

The transport of soil fumigant requires descriptions of the phase partition between liquid, gas and solid phase, dispersion (convection and diffusion), and degradation processes. Degradation was described using a first-order decay reaction, and included the ability to specify the degradation rate in each phase (liquid, vapor, and solid). The governing transport equations for the fumigant were written as follows (Šimůnek and van Genuchten, 1994):

$$\eta\frac{\partial C_g}{\partial t} + \theta\frac{\partial C_l}{\partial t} + \rho_b\frac{\partial C_s}{\partial t} = \frac{\partial}{\partial x}\left[D_g\frac{\partial C_g}{\partial x} + D_l\frac{\partial C_l}{\partial x} - q_x C_l\right] + \frac{\partial}{\partial z}\left[D_g\frac{\partial C_g}{\partial z} + D_l\frac{\partial C_l}{\partial z} - q_z C_l\right] - \eta\mu_g C_g - \theta\mu_l C_l - \rho_b\mu_s C_s \quad (3)$$

where C_g, C_l, and C_s are gas-, liquid-, and solid-phase concentrations ($\mu g\ cm^{-3}$), respectively; D_l and D_g are liquid- and gas-phase diffusion coefficients ($cm^2\ s^{-1}$), respectively; μ is a first-order degradation coefficient (s^{-1}); θ, ρ_b, and η, respectively, are water content ($cm^3\ cm^{-3}$), bulk density ($g\ cm^{-3}$), and air content ($cm^3\ cm^{-3}$); q is the Darcian flux density; and the subscripts: l, s, and g indicate liquid-, solid-, and gas-phases, respectively. The partitioning between the liquid- and gas-phase was assumed to obey Henry's Law (e.g., $C_g = K_h\ C_l$) and the partitioning between the liquid- and solid-phase was assumed to be equilibrium adsorption $C_s = K_d\ C_l$. The temperature dependence of the diffusion coefficients and degradation rates were described using

the Arrhenius Equation (e.g., $\mu(T) = \mu_r \exp[-E_a\,(T - T_r) / (R\,T\,T_r)]$), where μ_r and T_r are reference values, E_a is the activation energy, and R is the universal gas constant.

2.2. Volatilization

Jury et al. (1983) defined the soil surface-atmospheric mass transfer coefficient as

$$h = \frac{D_G^{air}}{b} \tag{4}$$

where D_G^{air} is the binary diffusion coefficient for the fumigant in air ($cm^2\ s^{-1}$) and is temperature dependent, and b (cm) is the a stagnant boundary layer thickness (often assumed to be 0.5 cm) and encompasses the processes occurring at the soil-atmosphere interface that affect fumigant emissions.

2.3. Modeling second-order reaction processes

Fumigant emissions can be reduced by enhancing degradation in soil by the addition of a reacting compound, such as ammonium thiosulfate (ATS). In several experiments (Gan et al., 1998a; Gan et al., 2000a), it was observed that many fumigants could be rapidly degraded in solutions or soils containing thiosulfate compounds. A proposed reaction mechanism was second-order, e.g.,

$$\omega_1 C_1 + \omega_2 C_2 \xrightarrow{k_{12}} \text{products} \tag{5}$$

where ω_i are stoichiometric coefficients, C_i are the concentrations of the fumigant and thiosulfate and k_{12} is the second-order reaction coefficient ($cm^3\ \mu mol^{-1}\ s^{-1}$). To simulate this reaction process requires adding an additional term to the right hand side of Eq. (3) to describe second-order loss (Yates and Enfield, 1988), that is:

$$\text{Second order loss} = -k_{12}\ C_{fumigant}\ C_{ATS} \tag{6}$$

The loss only occurs when both chemicals are present together in soil or solution and hence the two concentrations are multiplied together. This creates a nonlinear partial differential equation describing solute transport.

2.4. Field measurements

Five field experiments were conducted on a farm near Buttonwillow California to measure field-scale fumigant emissions for several management options; the details of these field experiments have been previously reported (Yates et al., 2008, 2011a, 2015, 2016, 2017). The fields were located approximately 25 miles west of Bakersfield, CA and about 5 miles NNE of Buttonwillow, California, in the San Joaquin Valley. The elevation is approximately 270–300 ft above mean sea level. USDA NRCS Soil Survey indicates that the soil in four of the five fields is classified as a Milham sandy loam soil, the exception was the treated portion of the northeast-most field site, which was classified as a Kimberlina fine sandy loam.

The experimental fields were prepared and managed by the grower according to standard practice and included irrigation, cultivation, preparation, fertilization, and pest control. Prior to the start of fumigation (approximately 1 week), the fields were prepared using a disk and ring roller or spiral packer. The fumigant was applied by a commercial applicator (Western Farm Services, Inc., Bakersfield, CA). The total mass applied to the field was calculated from measurements before and after application. Following application of the fumigants, the soil was sealed with a single pass of a disk and a ring roller in the direction of the shanks.

In 2005, two experiments were conducted to test if a surface water seal (Irrigation Treatment) and surface incorporation of composted municipal green waste material (Organic Matter Treatment) would reduce fumigant emissions compared to fumigations without a water seal or organic amendment. 1,3-D was applied at a rate of 12 gal/acre and at a depth of 46 cm (18 in.) to two fields in an identical manner. The Irrigation Treatment was then subjected to sequential sprinkler irrigations in which 1.3 cm water was sprayed onto the soil post-fumigation, and then again for the following four days approximately midday. The Organic Matter Treatment had composted municipal green waste applied and incorporated into the soil the previous year, which increased the fraction organic carbon from about 1% to 3.4%.

In 2007, a Standard Practice treatment and two additional emission-reduction approaches were tested which included deep-injection (i.e., 61 cm, Deep Injection Treatment) and spray application of ammonia thiosulfate fertilizer (ATS Treatment) to create a reactive surface barrier (Zheng et al., 2005). Telone C35 (65% 1,3-D and 35% chloropicrin) was applied to the three fields in an identical manner at a target rate of 20 gal/acre and at a depth of either 18 in. (46 cm; Standard Practice and ATS Treatments) or 24 in. (61 cm; Deep Injection Treatment). The Standard Practice treatment served as a control plot and did not have any other agronomic operation performed that would affect emissions. For the ATS Treatment, ATS solution was sprayed on to the field immediately after fumigation. Since the effect of thiosulfate concentration and surface-water sealing has already been shown to be effective in reducing 1,3-D emissions in laboratory experiments (Gan et al., 1998b; Gan et al., 2000a), the aim of this field experiment was determining the effectiveness of thiosulfate without water sealing in reducing field emissions. For the Deep Injection Treatment, only the injection depth differed from the Standard Practice Treatment.

There are several common methods for estimating the fumigant emissions from soils to the atmosphere, these methods include micrometeorological methods and regulatory "back-calculation" methods. For each experiment, three meteorological methods were used to estimate fumigant volatilization rates and total emission losses, which included: aerodynamic (ADM; Parmele et al., 1972), integrated horizontal flux (IHF; Denmead et al., 1977), theoretical profile shape (TPS; Wilson et al., 1982) methods. In addition, two regulatory "back-calculation" methods were used to measure the field emission rate and employed ISCST3 (Ross et al., 1996) or CALPUFF (Scire et al., 2000; CALPUFF v6.112, Earth Tech, Inc.). However, due to an equipment malfunction, only the flux rates calculated with ADM, CALPUFF and ISCST3 methods were available for all treatments and only these methodologies are used for comparisons with the simulations (Table 1 and Supporting information).

2.5. Numerical solutions to the transport equations

Hydrus1D version 4.14, Hydrus2D/3D version 1.11 (Šimůnek et al., 2008), and Solute1D (unpublished) were used to predict fumigant emission rates using various emission reduction strategies. The software programs were modified to include various fumigant-related processes, such as 2nd order reaction mechanisms, temperature dependent transport properties, the presence or absence of surface tarp, etc. These solution algorithms were used in a forward prediction mode based on the experimental parameters and fumigant properties at the time of the experiments (see Table S1). The results given below were obtained without using inverse or calibration approaches.

Since the Hydrus programs do not formally include a 2nd-order reaction mechanism, simulations of experiments that involved the use of ATS were obtained from Solute1D; which is a 1-D finite difference program that solves the water flow, heat and solute transport equations listed above. Simulations from this program have been compared to Hydrus and analytical solutions and were found to be equivalent (Yates, 2009). A comparison of Hydrus1D, Solute1D and the analytical solution is presented in Fig. S1 for two isomers of 1,3-D: 1,3-D (*cis*)

Table 1
Summary of total 1,3-D mass lost from emissions and percent of the applied fumigant lost for the Buttonwillow field experiments. The values from the aerodynamic (ADM), CALPUF, and ISCST3 methods.

Method	1,3-D (*cis*)		1,3-D (*trans*)		
	Peak emissions ($\mu g\ m^{-2}\ s^{-1}$)	Percent of applied Mass lost, %	Peak emissions ($\mu g\ m^{-2}\ s^{-1}$)	Percent of applied Mass lost, %	Percent of applied 1,3-D Mass lost, %
Standard Practice					
ADM	17.6	42.4	9.3	28.3	35.4
CALPUF	18.0	31.8	11.9	22.6	27.2
ISCST3	7.2	19.0	4.4	13.5	16.2
Avg (± std)	14.3 ± 6.1	31.1 ± 11.7%	8.5 ± 3.8	21.5 ± 7.5%	26.3 ± 9.6%
Irrigation Treatment					
ADM	30.9	17.5	28.9	13.1	15.3
CALPUF	5.6	12.2	3.9	8.6	10.0
ISCST3	4.3	7.8	2.8	5.4	6.6
Avg (± std)	13.6 ± 15	12.5 ± 4.9%	11.9 ± 14.8	9 ± 3.9%	10.6 ± 4.4%
Organic Matter Treatment					
ADM	10.0	9.7	13.2	6.6	8.2
CALPUF	4.1	4.7	2.8	3.2	4.0
ISCST3	2.9	3.0	1.4	1.8	2.5
Avg (± std)	5.6 ± 3.8	5.8 ± 3.5%	5.8 ± 6.5	3.9 ± 2.5%	4.3 ± 2.2
Deep Injection Treatment					
ADM	18.5	31.6	13.8	21.8	26.7
CALPUF	19.0	30.3	14.4	21.9	26.1
ISCST3	8.2	18.3	5.0	13.4	15.8
Avg (± std)	15.2 ± 6.1	26.7 ± 7.3%	11.1 ± 5.2	19 ± 4.9%	22.9 ± 6.1%
ATS Spray Treatment					
ADM	9.6	28.5	9.9	21.6	25.0
CALPUF	10.9	29.0	9.1	23.6	26.3
ISCST3	9.2	17.6	6.4	14.2	15.9
Avg (± std)	9.9 ± 0.9	25 ± 6.4%	8.4 ± 1.8	19.8 ± 5%	22.4 ± 5.7%

and 1,3-D (*trans*). Since the analytical solution requires restrictive assumptions concerning the soil and environmental properties that can be simulated, a comparison of the emissions of 1,3-D (*cis*) and 1,3-D (*trans*) from a point source is also shown in Fig. S2 using the initial and boundary conditions measured during the Standard Practice field study.

3. Model parameterization

3.1. Simulating field conditions

The simulations must be conducted using soil and environmental measurements reflective of experimental conditions to accurately simulate the emissions of 1,3-D. At the start of each experiment the soil temperature and soil water content were obtained at several depths in soil, which were used as initial condition input values for the simulations. For depths below the deepest measurement, it was assumed that the water content and soil temperature were constants, as shown in Fig. 1 for the Standard Practice field site. Water content and soil temperature was measured for each experiment and used as initial conditions for all treatments shown in Table 1. A summary of the other input parameters is provided in Table S1.

The initial 1,3-D concentration in soil was uniformly distributed along the shank injection zone from the depth of the injection port (i.e., 46 or 61 cm) to the bottom of the disked and rototilled surface layer (i.e., 20 cm). Visual inspection during the Standard Practice experiment showed that the surface layer was uniformly mixed and did not have evidence of a shank fracture zone (Fig. S3A), so 1-D simulations were conducted for all treatments under the assumption that fractures were not present.

The equipment used to inject the fumigants can lead to shank fractures within a soil profile (Fig. S3B) having a marked impact on the diffusion of the fumigants through the soil and volatilization into the atmosphere. A finite element grid was constructed to simulate a fracture-like opening in the soil (Fig. S4). This simulation is especially appropriate for the Deep Injection Treatment, since shank fractures were visually observed in an area within a few meters to the treated field (Fig. S3B). This involved using the injection rig, without applying the fumigant so trenching could be undertaken. Because the soil surface was disked following fumigant application, fractures were present only from the point of injection to a depth of approximately 20 cm. Since the existence of a soil fracture across the field would never be known, both 1-D and 2-D simulations were conducted so that the results would cover the range of the two limiting cases; i.e., presence and/or absence of shank fractures.

Surface boundary conditions during a simulation were described using time series of field measurements. A time series of evaporation rates at the soil surface (Fig. 2A) were calculated using micrometeorological

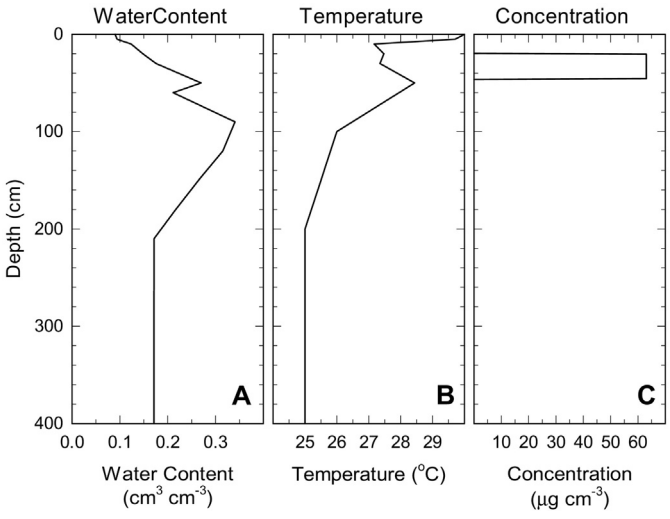

Fig. 1. Example of data used as initial values for the simulations. (A) is initial water content and (B) initial soil temperature measured in the Standard Practice field site. (C) is the soil concentration based on mass of 1,3-D applied and uniformly distributed from the injection depth (i.e., 46 cm) to the plow layer (i.e., 20 cm). The same distributions were used for 2-D simulations, but the concentration was uniformly distributed in the shank-disturbance zone (see Fig. S4).

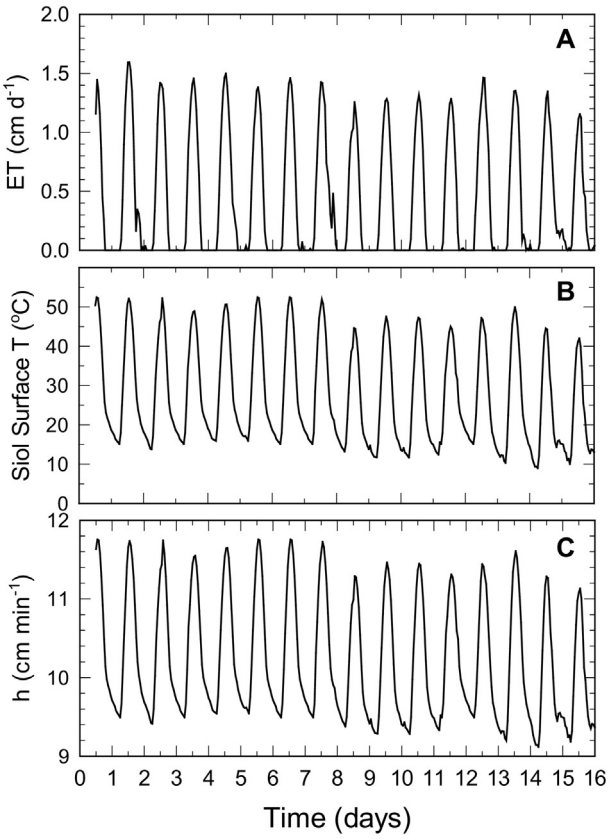

Fig. 2. (A) Penman evaporation rate (cm d^{-1}), (B) soil surface temperature (°C), and (c) mass transfer coefficient, h (cm min^{-1}) based on field measurements (Standard Practice field site). The values for h were obtained from Eq. (4) using the soil surface temperature.

measurements from the field experiment and the Penman equation (Allen et al., 1998). The field-measured evapotranspiration (ET) values compared well with published ET from the Belridge (Lost Hills) CMIS station located approximately 15 miles NW from the field site (<7% difference). Surface temperature measurements were collected near the center of the field (Fig. 2B) with an infrared thermometer and were used for the surface boundary condition in the temperature simulation. The 1,3-D mass transfer coefficient was calculated using surface temperatures and Eq. (4) (Fig. 2C). Free drainage/zero-gradient boundary conditions were simulated at 420 cm below the soil surface for water, heat and chemical transport.

Henry's law constants for 1,3-D (*cis*, $K_h = 0.074$) and 1,3-D (*trans*, $K_h = 0.043$) at 25 °C were obtained from Dow Agrosciences LLC (personal communication) and confirmed in laboratory experiments. The activation energy parameter for Henry's law constant was obtained by fitting the Arrhenius equation to the laboratory K_h measurements obtained from 5 to 40 °C (Fig. 3). The calculated activation energy was 34 kJ mol^{-1}. Soil degradation coefficients were calculated from laboratory data as reported by Ashworth and Yates (2007). For Milham sandy loam soil the first-order degradation rate was 5.3 d^{-1} and for the organic rich soil layer of the Organic Amendment field experiment the rate was 1.2 d^{-1}. The degradation activation energy (43 kJ mol^{-1}) was calculated from data reported by Gan et al. (1999). The activation energies for the binary gas and liquid diffusion coefficients were calculated by fitting the Arrhenius equation, respectively, to the Fuller, Schettler, Giddings and the Wilke-Chang correlations (Reid et al., 1987). The 2nd order rate constant, $k_{12} = 2.66E-6$ cm^3 mg^{-1} min^{-1}, was calculated from data reported by Gan et al. (2000b).

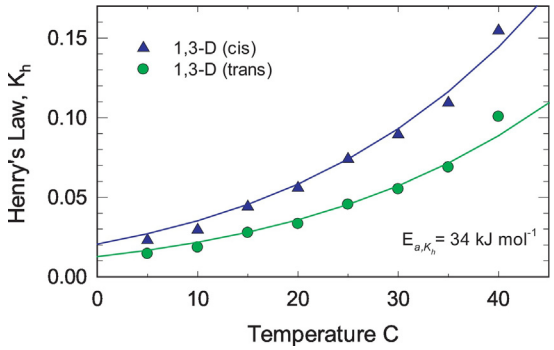

Fig. 3. Henry's law relationship for 1,3-D isomers as a function of temperature. Measured data are shown as triangles and circles. Solid lines are from the Arrhenius equation using $E_{a,Kh}$ of 34 kJ mol^{-1}.

4. Results & discussion

4.1. Field emissions measurement summary

Table 1 provides a summary of the field emission measurements used for comparison to the simulations. The results for the peak emission rate and total emissions for the 1,3-D (*cis*) and 1,3-D (*trans*) isomers and the total emissions for Telone II (50% *cis* + 50% *trans* 1,3-D), a common commercial formulation, are presented. In general, the ADM and CALPUFF methods produced higher emission rates compared to the ISCST3 method and for the 2007 experiments, the results from ADM and CALPUFF were similar. The ISCST3 method produced lower values that were often 50% or less than the other methods. The variations in the calculated emission rates are due, in part, to methodological differences, which can complicate model performance testing.

As shown for the Deep Injection Treatment (Fig. 4), graphically superimposing the emission-rate time series may not lead to clearly identifiable behaviors. Also, the diurnal cycle of the emission rate is not clearly visible. This is especially the case when the five flux calculation methods that were available for the Deep Injection Treatment are plotted (data not shown). The flux densities for the three methods that were available for all experimental treatments (i.e., ADM, CALPUFF, ISCST3) were averaged over the specific time periods to provide graphical information that more clearly shows the underlying process/behavior (Fig. 5). The advantages of averaging include reducing clutter, the daily cycles of the flux density becomes more apparent and the standard deviations can be computed.

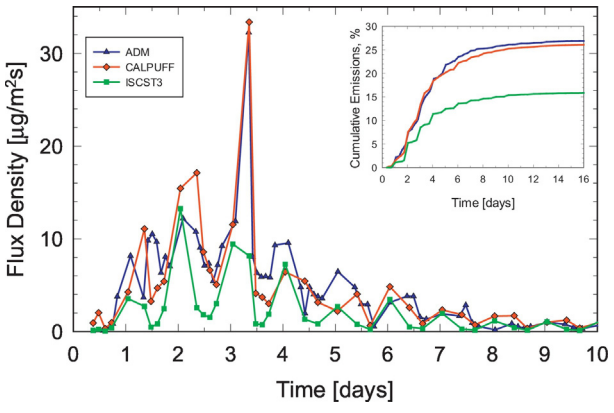

Fig. 4. Measured flux density during first 10 days of experiment for the Deep Injection experiment. The figure shows the similarity between ADM and CALPUFF emissions versus the IHF, TPS, and ISCST3 emissions, which are generally lower. All flux calculation methods are shown. Timescale begins at midnight 9/5/2007.

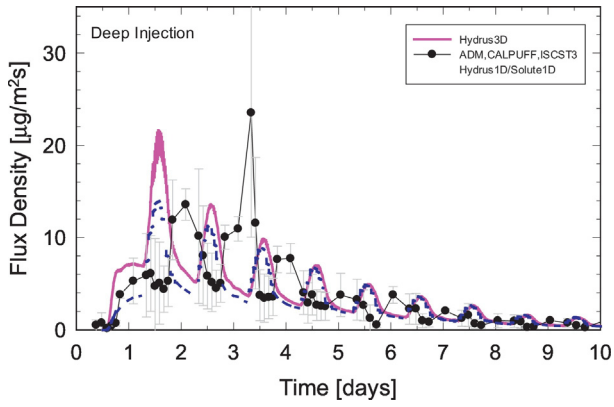

Fig. 5. Measured flux density from ADM, CALPUFF and ISCST3 methods for Deep Injection field. Error bars are standard deviations. The lines are the simulated flux density using Hydrus3D or using 1-D models (i.e., Hydrus1D or Solute1D; the 1-D models produce identical results).

4.2. Predicted emissions

4.2.1. Deep Injection Treatment (2007)

Predicted emissions (i.e., flux density) values using 2-D (Hydrus2D/3D) and 1-D models (i.e., Hydrus1D/Solute1D) for the Deep Injection Treatment are shown in Fig. 5. To accurately simulate 1,3-D (*cis* + *trans*), the simulations of each isomer must be conducted and the results combined since differences in K_h between isomers causes differences in transport and emission rate. The main difference between 2-D and 1-D models is the 2-D model simulates a shank fracture from the injection depth to 20 cm below the soil surface (Figs. S3B and S4). The 1-D models assume a line source extending from the injection depth to 20 cm from the soil surface (Fig. 1C).

With the exception of the high flux rate at 3-days, the predicted flux density is similar in magnitude to measurements over the course of the experiment. However, the model does not adequately predict the timing of the peak daily flux density values. All the model simulations predict the peak emissions at mid-day, in accordance with the theoretical underpinnings of the modeling approach; where gas transport and surface mass transport increases with temperature. However, after several days the field measurements clearly show that the highest emission rates occur during the nighttime or early morning hours. This behavior was observed in all of the experiments and all flux calculation methods. Similar results were also reported by Cryer and van Wesenbeeck (2010) for a 2-D modeling study that included six field trials conducted in five states.

The predictions using 2-D and/or 1-D models captures the general trend in the emission rates, with large emission loss cycles early in the experiment that dissipate by 10 days. The 2-D model simulates the shank fracture that was observed during this field experiment, and a visual inspection of Fig. 5 shows a better overall match of the peak values over the course of the experiment than the 1-D models, which tended to underestimate the cumulative magnitude of the first two peak emission rates.

The averaged (1-D & 2-D) simulated peak emissions for 1,3-D (*cis*) and 1,3-D (*trans*) were 13.6 ± 6.3 and 7.5 ± 3.8 µg m^{-2} s^{-1}, respectively, for the Deep Injection Treatment (Table 2). This compares to 18.4 ± 4.9 and 11.1 ± 4.3 µg m^{-2} s^{-1} for the simulated Standard Practice treatment (Fig. S5) revealing that, based on simulated values, Deep Injection reduces peak emissions by 26% (*cis*) and 32% (*trans*) when compared to a standard injection depth (i.e., 46 cm) simulations. An opposing result was observed for the field measurements (Table 1), where the Deep

Table 2
Summary of the simulated total 1,3-D mass lost from emissions and percent of the applied fumigant lost for the Buttonwillow field experiments. The values from the analytical solution, 2-D simulation (Hydrus3D), and 1-D simulations: Hydrus 1D (H1D) and Solute (S1D).

Experimental treatment	1,3-D (*cis*)			1,3-D (*trans*)			1,3-D
	Peak emissions (µg m^{-2} s^{-1})	Total emissions %	Total degrad %	Peak emissions (µg m^{-2} s^{-1})	Total emissions %	Total degrad %	Total emissions %
Standard Practice							
Analytical	13.8	32%	68%	7.3	23%	77%	26%
Hydrus3D	21.9	38%	61%	14.1	27%	72%	33%
H1D, S1D	14.9	30%	68%	8.1	21%	77%	25%
Avg (± std)[a]	18.4 ± 4.9	34.1 ± 5.5%	64.6 ± 4.5%	11.1 ± 4.3	23.9 ± 4.8%	74.3 ± 3.6%	29 ± 5.2%
Irrigation Treatment							
Analytical	8.3	28%	72%	4.3	19%	81%	22%
Hydrus3D	3.9	11%	86%	1.5	5.7%	91%	8.3%
H1D, S1D	2.9	4.7%	91%	0.73	1.9%	94%	3%
Avg (± std)[a]	3.4 ± 0.7	7.8 ± 4.4%	88.9 ± 3.5%	1.1 ± 0.5	3.8 ± 2.7%	92.6 ± 1.6%	5.8 ± 3.5%
Organic Matter Treatment							
Analytical	3.5	4.8%	95%	1.3	2.1%	98%	3.5%
Hydrus3D	10.4	14%	87%	4.7	6.9%	94%	11%
H1D, S1D	2.7	5.2%	94%	0.9	1.9%	97%	3.5%
Avg (± std)	8.9 ± 2.1	12.8 ± 2%	87.3 ± 1%	3.8 ± 1.3	6 ± 1.2%	94.2 ± 0%	9.4 ± 1.6%
Deep Injection Treatment							
Analytical	9.0	26%	74%	4.7	18%	82%	21%
Hydrus3D	18.1	28%	70%	10.1	19%	78%	24%
H1D, S1D	9.2	22%	75%	4.8	15%	82%	18%
Avg (± std)[a]	13.6 ± 6.3	25.1 ± 3.9%	72.4 ± 3.5%	7.5 ± 3.8	16.8 ± 3.3%	80.3 ± 2.8%	21 ± 3.6%
ATS Spray Treatment[b]							
$k_{12} = 0$							
Analytical	13.1	31%	69%	6.96	22%	78%	26%
Hydrus3D	22.8	34%	66%	14.0	25%	76%	29%
H1D, S1D	33.3	28%	71%	16.9	19%	80%	25%
Avg (± std)[a]	28.1 ± 7.5	31.2 ± 4.1%	68.5 ± 3.1%	15.4 ± 2	22.1 ± 3.7%	77.7 ± 2.6%	27.2 ± 3.2%
$k_{12} = 0.0038$ cm ^{3} µg^{-1} d^{-1}							
S1D, k_{12} constant	30.7	26%	73%	15.3	17%	82%	21%
S1D, k_{12} (T)	27.7	23%	76%	13.0	14%	85%	19%
Avg (± std)	29.2 ± 2.2	24.4 ± 2%	74.7 ± 2%	14.1 ± 1.6	15.5 ± 2%	83.5 ± 2%	19.9 ± 2%

[a] Average and standard deviations do not include the analytical solution.
[b] Incorporation depth 10 cm.

Injection 1,3-D (*cis*) and 1,3-D (*trans*) peak emissions for the average of the ADM, CALPUFF and ISCST3 methods were 15.2 ± 6.1 (*cis*) and 11.1 ± 5.2 (*trans*) μg m^{-2} s^{-1}, respectively. The measurements reveal that measured Deep Injection peak emissions were 6.3% (*cis*) and 30.6% (*trans*) higher than the Standard Practice measurements, which is likely due to the presence of the shank fractures. This experimental result can be further investigated by comparing the simulated Deep Injection (2-D simulation, with 18.1 (*cis*) and 10.1 (*trans*) μg m^{-2} s^{-1}) to the simulated Standard Practice (1-D, with 14.9 (*cis*) and 8.1 (*trans*) μg m^{-2} s^{-1}) which shows the peak emissions for the Deep Injection were 21.5% (*cis*) and 24.7% (*trans*) higher than the Standard Practice. This analysis suggests the importance of the shank fracture, when they are present after soil fumigation, suggesting that the fracture could have served as a preferential pathway for 1,3-D transport through soil. Also, the improved match of the 1-D simulation for the Standard Practice treatment (Fig. S5) suggests that soil fractures were not a significant feature of the Standard Practice treatment, which conforms with visual observations adjacent to the field site (Fig. S3A).

The analytical solution provides a simple means for simulating emissions, which for the Standard Practice and Deep Injection Treatments provide similar results to the numerical simulation (Table 2). The similarity between the peak and total emission for the analytical solution and the 1-D simulation is likely a reflection of using parameter values that represent the average temperature during the experiment, the limited water movement, and the relatively uniform soil properties compared to other treatments. For these two treatments using an analytical solution to obtain total emissions appears to be appropriate.

4.2.2. ATS Treatment (2007)

The importance of the 2nd order reaction process when ATS is applied to a field fumigated with 1,3-D is apparent (Fig. 6). The 2-D and 1-D simulations where $k_{12} = 0$ (Fig. 6A) significantly over-predict the early-time measurements. The Solute1D simulations shown in Fig. 6B includes a 2nd-order reaction process (with k_{12} = 0.0038 cm^3 μg^{-1} d^{-1} in Eq. (6)) and has a peak 1,3-D emission rate of 20.3 μg m^{-2} s^{-1}, compared to 24.9 μg m^{-2} s^{-1} when the 2nd order reaction is not simulated. The second-order reaction process corresponds more closely to the measured emission rates but also overestimates the early measurements. Simulating the 2nd order reaction process also leads to a 7% reduction in percent total emissions (i.e., 27% to 20%). Similar behavior was observed in the field measurements where the total 1,3-D emissions for the ATS Treatment were 22.4 ± 5.7%, while the Standard Practice treatment had total emissions of 26.3 ± 9.6% (Table 1), which is a 4% reduction in percent total emissions. Shank fractures were not visually observed in a test area adjacent to this field site. In general, the 2-D model predicted higher emissions than the 1-D model (up to 10 μg m^{-2} s^{-1}, Fig. 6A with $k_{12} = 0$). Including the 2nd order reaction mechanism in the 1-D model (Fig. 6B) reduced the flux density by 2–5 μg m^{-2} s^{-1}compared to the 1-D model without 2nd order reaction. A comparison of both curves (Fig. 6A–B) suggests that the 2-D model would likely still overestimate the emission rate if the 2nd order reaction mechanism could be simulated and is evidence that fractures were not a significant feature in the treated area of the field.

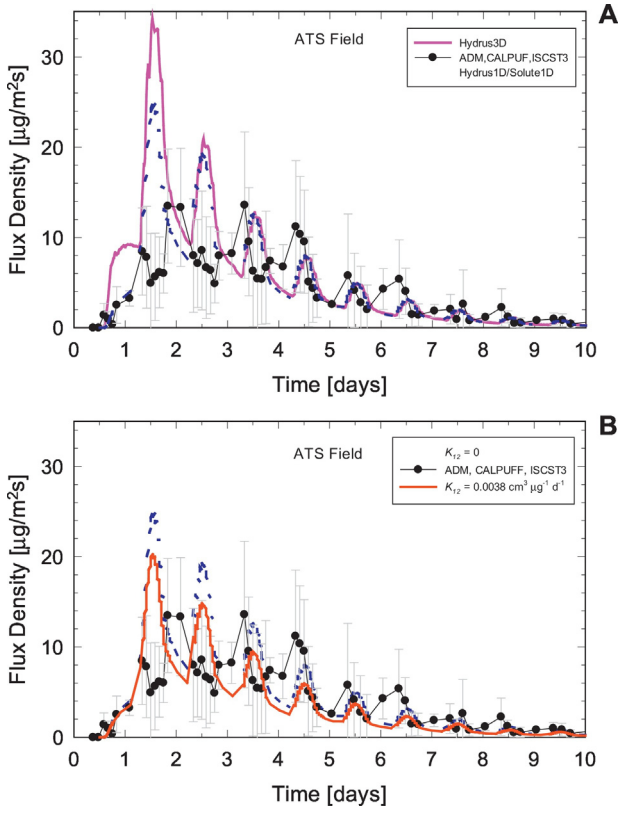

Fig. 6. Simulated and measured flux density (μg m^{-2} s^{-1}) in ATS field. In (A), Hydrus simulations with $k_{12} = 0$. In (B) 1-D simulations with $k_{12} = 0$ and k_{12} = 0.0038 cm^3 μg^{-1} d^{-1}. Error bars are standard deviations.

The total 1,3-D emission for the standard practice (29.0 ± 5.2%), was similar to that of the ATS Spray treatment (27.2 ± 3.2%) when the second-order reaction process was not simulated (i.e., $k_{12} = 0$). However, not simulating the 2nd order process overestimated the measured total emissions (22.4 ± 5.7%, Table 1) by 21%. Simulating the second-order reaction process resulted in total emissions (19.9 ± 2.0%) that were 11% lower than the observed total emissions for this experiment. Using a constant k_{12} appears to more accurately simulate the measured emissions when contrasted with a temperature-dependent value (21% vs. 19%).

For the ATS Treatment, the analytical solution used a spatially-weighted first-order degradation rate for the simulation. While using a weighted degradation rate produced a value for the total emissions that was the very similar to the 1-D numerical simulations, the solution under-predicted the peak emission rate. However, simulating the 2nd order reaction process produces a nonlinear partial differential equation that cannot be solved analytically and would require a numerical solution. Also, differences between the analytical and 1-D solutions show that the analytical solution may not be appropriate for simulating this treatment.

4.2.3. Organic Matter Treatment (2005)

The most significant difference between the Organic Matter Treatment and the Standard Practice Treatment was a higher first-order soil degradation rate constant (0.0241 h^{-1}) measured in the surface soil (0–20 cm) which was due to the application and incorporation of composted organic municipal green waste material the previous year. The higher level of organic matter also had an effect on the fraction organic carbon and the sorption coefficient (0.85 cm^3 g^{-1}) compared to the native soil from the Standard Practice experiment (0.25 cm^3 g^{-1}).

The peak measured emission rate for 1,3-D (*cis*: 5.6 ± 3.8; *trans*: 5.8 ± 6.5 (μg m^{-2} s^{-1}) and total 1,3-D emissions (4.3 ± 2.2%) are shown in Table 1 and Fig. S6 and compare well to the non-fracture (1-D) model simulations shown in Table 2 (*cis*: 2.7 μg m^{-2} s^{-1}; *trans*: 0.9 μg m^{-2} s^{-1}; total 1,3-D emissions 3.5%). These values also compare well to a laboratory study where peak emissions of 1,3-D (*cis*) were 2.8 ± 0.82 μg m^{-2} s^{-1} and total emissions were found to be 5.7%, of the applied *cis* isomer of 1,3-D (Ashworth and Yates, 2007). The 2-D simulation overestimated these values by as much as a factor of approximately 3. For this treatment, the analytical solution produced values for the peak and total emissions that were very similar to those of the 1-D numerical simulations. For this treatment, the use of a depth-weighted first-order degradation rate (see Table S2, footnote *i*) appears appropriate and provides a simple means for estimating total emissions.

4.2.4. Irrigation Treatment (2005)

For the Irrigation Treatment, water was applied to the soil surface at midday on the day of application and each of the following 4 days to create a diffusion barrier by filling the soil pores with water. The effect of a water seal is clearly seen in the measured emission rates shown in Table 1 (and Fig. S7), with total emission approximately 60% less than the Standard Practice treatment. The Irrigation Treatment did not appreciably reduce the averaged peak emission rate, which was significantly influenced by the large values calculated with the ADM.

The simulation significantly underestimated the emission rates at early times and overestimated emission rate at later times (Fig. S7). After about 5 days, the peak field measured emission rates were less than about 1.5 $\mu g\ m^{-2}\ s^{-1}$ and the simulated values were as high as 3.0 $\mu g\ m^{-2}\ s^{-1}$ and continued to exceed 1.0 $\mu g\ m^{-2}\ s^{-1}$ for another 5 days, whereas the field measurements quickly approached nearly zero. The field results were also similar to a column experiment that was conducted with the same soil and conditions of this field study (Ashworth and Yates, 2007). The laboratory column study found that the peak 1,3-D (*cis*) emissions were 5.6 ± 0.34 $\mu g\ m^{-2}\ s^{-1}$, which is similar to the peak 1,3-D (*cis*) emissions of the CALPUFF and ISCST3 back calculation methods. The total 1,3-D (*cis*) emissions in the laboratory experiment were 17.1% and the field value for the total emissions of 12.5 ± 4.9%. It is unclear why the simulations underestimated the measured peak and total emission rates, but this result suggests that the model does not capture all of the processes important in describing fumigant emissions when the soil surface is irrigated.

The analytical solution is not able to simulate water movement, so the higher total emissions, and similarity to the Standard Practice (i.e., minimal water movement), are expected. The results from the analytical solution were included here for completeness, but are clearly not representative of the experiments with irrigation.

4.2.5. Emission timing

Most of the numerical simulations predicted the maximum emission rate at about 1.5 days. The measurements, however, revealed the maximum emission rate occurring usually at about 3 days. One exception was the Irrigation Treatment where the addition of irrigation water created a surface water seal that significantly reduced 1,3-D emissions early in the experiment and larger emissions after irrigation ceased. No clear explanation was found for the delayed maximum emission in the field measurements compared to the simulations. This is another area that requires additional research.

The measured daily peak emission rates occur about ⅓–½ day earlier than the simulations. The measurements were likely affected by changes in the soil water content at the surface, where heating and turbulence creates drying conditions near midday. When very dry soil conditions occur, vapor adsorption can increase, which reduces the vapor density and the associated gradients (Spencer et al., 1969; Glotfelty et al., 1984; Reichman et al., 2011). It has been shown that vapor phase adsorption increases when the water content decreases below a threshold level (Spencer and Cliath, 1973) for a volatile insecticide. The significance of vapor adsorption has been confirmed for 1,3-D in recent laboratory experiments (unpublished data). Vapor adsorption has been shown to strongly bind volatile pesticides to soil particles in a highly nonlinear process (Reichman et al., 2013a, 2013b). Since the commonly available numerical models do not simulate the effects of soil water content on vapor adsorption of fumigants, these models predict high mid-day emission values when temperatures are greatest.

5. Conclusions

The agreement between the measured and simulated emission fluxes varied considerably based on the method used to calculate the flux density field measurements. It is not possible to determine simulation model accuracy using this dataset since a method for showing which flux calculation method produces the most accurate flux density values is lacking. While it is not possible to determine which calculation method is most accurate, inspection of each method's inherent assumptions may provide an indication of the potential accuracy of each method. For example, the ISCST3 method assumes steady-state atmospheric dispersion during hourly time periods. It is unlikely the ISCST3 flux density values are the most accurate given the high temporal variability of the wind speed and wind direction that can occur during an experiment. CALPUFF is a Lagrangian puff model that tracks chemical movement in a relatively natural manner and can be used for high frequency and temporally variable conditions. The back-calculation methods using CALPUFF likely provides more accurate flux density values compared to using ISCST3 (i.e., steady state), but the results depend on the grid system choice as well as the representativeness of the meteorological data. The ADM method is a direct method to calculate the flux density and assumes that gradients (concentration, wind speed and temperature) near the surface are fully developed. However, the ADM requires evaluation of a correction term for stable and unstable atmospheric conditions, which may introduce uncertainty and/or bias. Lack of a clearly superior approach for measuring field-scale emissions makes quantifying the accuracy of the simulation results problematic.

The study results seemed consistent given the experimental uncertainty for measuring emissions of methyl bromide using the ADM, which was reported by Majewski (1997) to be about ± 50%. This analysis was based on a linear regression of the log-linear wind speeds and concentrations with respect to height so the results should also apply to 1,3-D emissions. The theoretical accuracy of the integrated horizontal flux method was determined to be within approximately 20% for appropriately large field sites and surface roughness lengths below 10 cm using a Lagrangian stochastic model (Wilson and Shum, 1992), so a range of 20–50% accuracy seems reasonable. Simulation of the field-scale emission experiments resulted in total emission predictions that were reasonably accurate and were generally within approximately 5–10% of measured values. This is easily within the accuracy range for these flux calculation methods.

In many situations, the total emission losses are of interest even though simulation results miss the observed peak 1,3-D emission rates. Based on the 1,3-D simulation averages shown in Table 2 (last column), the highest total 1,3-D emission observed was for the Standard Practice treatment (29.0 ± 5.2%). Overall trends in total emissions are consistent with measurements: Standard Practice > Deep Injection (28%) ~ ATS Spray (31%) > Organic Matter (76%) ~ Irrigation (80%).

Acknowledgements

The use of trade, firm, or corporation names in this research article is for the information and convenience of the reader. Such use does not constitute an official endorsement or approval by the United States Department of Agriculture or the Agricultural Research Service of any product or service to the exclusion of others that may be suitable. USDA is an equal opportunity provider and employer. The research described was supported by USDA ARS (Project No. 2036-12130-011-00D) and California Air Resources Board (Agreement #05-351).

Appendix A. Supplementary data

A table of soil and chemical properties used in the simulations; a comparison of Hydrus1D, Solute1D and an analytical solution for isothermal, no water flow conditions; a comparison of Hydrus1D and Solute1D for *cis*-1,3-D and *trans*-1,3-D for the Standard Practice experiment; pictures showing presence and absence of shank fractures; a graph of the grid system for the Hydrus2D/3D simulations; comparison of Hydrus2D/3D simulations and measured emission rates for the Standard Practice, Organic Matter, and Irrigation scenarios. This information is available free of charge via the Internet at http://pubs.acs.org. Supplementary data to this article can be found online at https://doi.org/10.1016/j.scitotenv.2017.11.278.

References

Albrecht, W.N., 1987. Occupational exposure to 1,3-dichloropropene (Telone) in Hawaiian pineapple culture. Arch. Environ. Health 42, 286–291.

Allen, R.G., Pereira, L.S., Raes, D., Smith, M., 1998. Crop Evapotranspiration–Guidelines for Computing Crop Water Requirements, FAO Irrigation and Drainage Paper 56. FAO-Food and Agriculture Organization of the United Nations, Rome, Italy (293 pp.).

Ashworth, D.J., Yates, S.R., 2007. Surface irrigation reduces the emission of volatile 1,3-dichloropropene from agricultural soils. Environ. Sci. Technol. 41, 2231–2236.

Ashworth, D.J., Ernst, F., Xuan, R., Yates, S.R., 2009. Laboratory assessment of emission reduction strategies for the agricultural fumigants 1,3-dichloropropene and chloropicrin. Environ. Sci. Technol. 43, 5073–5078.

Baker, L.W., Fitzell, D.L., Seiber, J.N., Parker, T.R., Shibamoto, T., Poor, M.W., Longley, K.E., Tomlin, R.P., Propper, R., Duncan, D.W., 1996. Ambient air concentrations of pesticides in California. Environ. Sci. Technol. 30, 1365–1368.

Basile, M., Senesi, N., Lamberti, F., 1986. A study of some factors affecting volatilization losses of 1,3-dichloropropene (1,3-D) from soil. Agric. Ecosyst. Environ. 17, 269–279.

CDPR (California Department of Pesticides Regulation), January 30, 2002. California Management Plan: 1,3-Dichloropropene. Department of Pesticide Regulation, Sacramento, CA http://www.cdpr.ca.gov/docs/emon/methbrom/telone/mgmtplan.pdf.

CDPR (California Department of Pesticides Regulation), 2017. Summary of Pesticide Use Report Data 2015 Indexed by Chemical. (Sacramento, CA). Available at:. http://www.cdpr.ca.gov/docs/pur/pur15rep/chmrpt15.pdf.

Chellemi, D.O., Ajwa, A., Sullivan, D., 2010. Atmospheric flux of agricultural fumigants from raised-bed, plastic-mulch crop production systems. Atmos. Environ. 44, 5279–5286.

Chen, C., Green, R.E., Thomas, D.M., Knuteson, J.A., 1995. Modeling 1,3-dichloropropene vapor-phase advection in the soil profile. Environ. Sci. Technol. 29, 1816–1821.

Cryer, S.A., van Wesenbeeck, I.J., 2010. Estimating field volatility of soil fumigants using CHAIN-WD: mitigation methods and comparison against chloropicrin and 1,3-dichloropropene field observations. Environ. Model. Assess. 15, 309–318.

Denmead, O.T., Simpson, J.R., Freney, J.R., 1977. A direct field measurement of ammonia emission after injection of anhydrous ammonia. Soil Sci. Soc. Am. J. 41, 1001–1004.

Gan, J., Yates, S.R., Crowley, D., Becker, J.O., 1998a. Acceleration of 1,3-dichloropropene degradation by organic amendments and potential application for emissions reduction. J. Environ. Qual. 27, 408–414.

Gan, J., Yates, S.R., Wang, D., Ernst, F.F., 1998b. Effect of application methods on 1,3-dichloropropene volatilization from soil under controlled conditions. J. Environ. Qual. 27, 432–438.

Gan, J., Papiernik, S.K., Yates, S.R., Jury, W.A., 1999. Temperature and moisture effects on fumigant degradation in soil. J. Environ. Qual. 28, 1436–1441.

Gan, J., Becker, J.O., Ernst, F.F., Hutchinson, C., Yates, S.R., 2000a. Surface application of ammonium thiosulfate fertilizer to reduce volatilization of 1,3-dichloropropene from soil. Pest Manag. Sci. 56, 264–270.

Gan, J., Becker, J.O., Ernst, F.F., Hutchinson, C., Yates, S.R., 2000b. Transformation of 1,3-dichloropropene in soil by thiosulfate fertilizers. J. Environ. Qual. 29, 1476–1481.

Gao, S., Trout, T.J., 2007. Surface seals reduce 1,3-dichloropropene and chloropicrin emissions in field tests. J. Environ. Qual. 36, 110–119.

Gao, F., Yates, S.R., Yates, M.V., Gan, J., Ernst, F.F., 1997. Design, fabrication, and application of a dynamic chamber for measuring gas emissions from soil. Environ. Sci. Technol. 31, 148–153.

Gao, S., Trout, T.J., Schneider, S., 2008. Evaluation of fumigation and surface seal methods on fumigant emissions in an orchard replant field. J. Environ. Qual. 37, 369–377.

Gao, S., Qin, R., Hanson, B.D., Tharayil, N., Trout, T.J., Wang, D., Gerik, J., 2009. Effects of manure and water applications on 1,3-dichloropropene and chloropicrin emissions in a field trial. J. Agric. Food Chem. 57, 5428–5434.

Glotfelty, D.E., Taylor, A.W., Turner, B.C., Zoller, W.H., 1984. Volatilization of surface-applied pesticides from fallow soil. J. Agric. Food Chem. 32, 638–643.

Jury, W.A., Horton, R., 2004. Soil Physics. 6th edition. John Wiley & Sons, Inc., Hoboken, New Jersey (384 pp.).

Jury, W.A., Spencer, W.F., Farmer, W.J., 1983. Behavior assessment model for trace organics in soil: 1. Model description. J. Environ. Qual. 12, 558–564.

Majewski, M.S., 1997. Error evaluation of methyl bromide aerodynamic flux measurements. In: Seiber, J.N., et al. (Eds.), Fumigants: Environmental Fate, Exposure, and Analysis. ACS Symposium Series 652. American Chemical Society, Washington, DC, pp. 135–153.

McDonald, J.A., Gao, S., Qin, R., Thomas, J., 2008. Thiosulfate and manure amendment with water application and tarp on 1,3-dichloropropene emission reductions. Environ. Sci. Technol. 42, 398–402.

Neal, R., Spurlock, F., Segawa, R., 2009. Annual report on volatile organic chemical emissions from pesticides: emissions for 1990–2007. Report EH09-01 (March 2009). California Environmental Protection Agency, Sacramento, CA (39 pp.).

Parmele, L.H., Lemon, E.R., Taylor, A.W., 1972. Micrometeorological measurement of pesticide vapor flux from bare soil and corn under field conditions. Water Air Soil Pollut. 1, 433–451.

Reichman, R., Rolston, D.E., Yates, S.R., Skaggs, T.H., 2011. Diurnal variation of diazinon volatilization: soil moisture effects. Environ. Sci. Technol. 45, 2144–2149.

Reichman, R., Yates, S.R., Skaggs, T.H., Rolston, D.E., 2013a. Effects of soil moisture on the diurnal pattern of pesticide emission: numerical simulation and sensitivity analysis. Atmos. Environ. 66, 41–51.

Reichman, R., Yates, S.R., Skaggs, T.H., Rolston, D.E., 2013b. Effects of soil moisture on the diurnal pattern of pesticide emission: comparison of simulations with field measurements. Atmos. Environ. 66, 52–62.

Reid, R.C., Prausnitz, J.M., Poling, B.E., 1987. The Properties of Gases and Liquids. 4th ed. McGraw-Hill, New York (741 pp.).

Ross, L.J., Johnson, B., Kim, K.D., Hsu, J., 1996. Prediction of methyl bromide flux from area sources using the ISCST3 model. J. Environ. Qual. 25, 885–891.

Scire, J.S., Strimaitis, D.G., Yamartino, R.J., 2000. User's Guide for the CALPUFF Dispersion Model. Earth Tech, Inc., Concord, MA (521 pp.).

Šimůnek, J., van Genuchten, M.Th., 1994. The CHAIN-2D code for simulating the two-dimensional movement of water, heat, and multiple solutes in variably-saturated porous media. Version 1.1, Research Report No. 136. U.S. Salinity Laboratory, USDA-ARS, Riverside, CA (194 pp.).

Šimůnek, J., van Genuchten, M.Th., Šejna, M., 2008. Development and applications of the HYDRUS and STANMOD software packages, and related codes. Vadose Zone J. 7, 587–600.

Spencer, W.F., Cliath, M.M., 1973. Pesticide volatilization as related to water loss from soil. J. Environ. Qual. 2, 284–289.

Spencer, W.F., Cliath, M.M., Farmer, W.J., 1969. Vapor density of soil-applied dieldrin as related to soil-water content, temperature, and dieldrin concentration. Soil Sci. Soc. Am. Proc. 33, 509–511.

van den Berg, F., 1992. Measured and computed concentrations of 1,3-dichloropropene in the air around fumigated fields. Pestic. Sci. 36, 195–206.

van den Berg, F., Kubiak, R., Benjey, W., Majewski, M., Yates, S.R., Reeves, G., Smelt, J., van der Linden, A., 1999. Emission of pesticides into the air. Water Air Soil Pollut. 115, 195–218.

van Wesenbeeck, I., Knuteson, J.A., Barnekow, D.E., Phillips, A.M., 2007. Measuring flux of soil fumigants using the aerodynamic and dynamic flux chamber methods. J. Environ. Qual. 36, 613–620.

Wauchope, R.D., Buttler, T.M., Hornsby, A.G., Augustijn-Beckers, P.W.M., Burt, J.P., 1992. The SCS/ARS/CES pesticide properties database for environmental decision-making. Rev. Environ. Contamin. Toxicol. Springer-Verlag 123, 1–155.

Wilson, J.D., Shum, W.K.N., 1992. A re-examination of the integrated horizontal flux method for estimating volatilisation from circular plots. Agric. For. Meteorol. 57, 281–295.

Wilson, J.D., Thurtell, G.W., Kidd, G.E., Beauchamp, E.G., 1982. Estimation of the rate of gaseous mass transfer from a surface source plot to the atmosphere. Atmos. Environ. 16 (8), 1861–1867.

Yates, S.R., 2009. Analytical solution describing pesticide volatilization from soil affected by a change in surface condition. J. Environ. Qual. 38, 259–267.

Yates, S.R., Enfield, C.G., 1988. Decay of dissolved substances by second-order reaction. Problem description and batch reactor solutions. J. Environ. Sci. Health Part A Environ. Sci. Eng. A23, 59–84.

Yates, S.R., Knuteson, J., Ernst, F.F., Zheng, W., Wang, Q., 2008. The effect of sequential surface irrigations on field-scale emissions of 1,3-dichloropropene. Environ. Sci. Technol. 42, 8753–8875.

Yates, S.R., Knuteson, J., Zheng, W., Wang, Q., 2011a. Effect of organic material on field-scale emissions of 1,3-dichloropropene. J. Environ. Qual. 40, 1470–1479.

Yates, S.R., McConnell, L.L., Hapeman, C.J., Papiernik, S.K., Gao, S., Trabue, S.L., 2011b. Managing agricultural emissions to the atmosphere: state of the science, fate and mitigation, and identifying research gaps. J. Environ. Qual. 40, 1347–1358.

Yates, S.R., Ashworth, D.J., Zheng, W., Zhang, Q., Knuteson, J., van Wesenbeeck, I.J., 2015. Emissions of 1,3-dichloropropene and chloropicrin after soil fumigation under field conditions. J. Agric. Food Chem. 63, 5354–5363.

Yates, S.R., Ashworth, D.J., Zheng, W., Knuteson, J., van Wesenbeeck, I.J., 2016. Effect of deep injection on field-scale emissions of 1,3-dichloropropene and chloropicrin from bare soil. Atmos. Environ. 137, 135–145.

Yates, S.R., Ashworth, D.J., Zhang, Q., 2017. Effect of surface application of ammonium thiosulfate on field-scale emissions of 1,3-dichloropropene. Sci. Total Environ. 580, 316–323.

Zheng, W., Papiernik, S.K., Guo, M., Dungan, R.S., Yates, S.R., 2005. Construction of a reactive surface barrier to reduce fumigant 1,3-dichloropropene emissions. Environ. Toxicol. Chem. 24, 1867–1874.

Zheng, W., Yates, S.R., Papiernik, S.K., Wang, Q.Q., 2006. Reducing 1,3-dichloropropene emissions from soil columns amended with thiourea. Environ. Sci. Technol. 40, 2402–2407.